Chemical Science

ROYAL SOCIETY OF CHEMISTRY

EDGE ARTICLE

View Article Online
View Journal | View Issue

Cite this: *Chem. Sci.*, 2020, **11**, 1114

All publication charges for this article have been paid for by the Royal Society of Chemistry

Self-sorting of two imine-based metal complexes: balancing kinetics and thermodynamics in constitutional dynamic networks†

Jean-François Ayme[ab] and Jean-Marie Lehn *[ab]

A major hurdle in the development of complex constitutional dynamic networks (CDNs) is the lack of strategies to simultaneously control the output of two (or more) interconnected dynamic processes over several species, namely reversible covalent imine bond formation and dynamic metal–ligand coordination. We have studied in detail the self-sorting process of 11 constitutional dynamic libraries containing two different amines, aldehydes and metal salts into two imine-based metal complexes, having no overlap in terms of their compositions. This study allowed us to determine the factors influencing the fidelity of this process (concentration, electronic and steric parameters of the organic components, and nature of the metal cations). In all 11 systems, the outcome of the process was primarily determined by the ability of the octahedral metal ion to select its pair of components from the initial pool of components, with the composition of the weaker tetrahedral complex being imposed by the components rejected by the octahedral metal ions. Different octahedral metal ions required different levels of precision in the "assembling instructions" provided by the organic components of the CDN to guide it towards a sorted output. The concentration of the reaction mixture, and the electronic and steric properties of the initial components of the library were all found to influence the lifetime of unwanted metastable intermediates formed during the assembling of the two complexes.

Received 4th October 2019
Accepted 4th December 2019

DOI: 10.1039/c9sc04988f

rsc.li/chemical-science

Introduction

Rivalling with the intricacy of biological processes in the construction and the exploitation of complex networks of molecules requires the development of new synthetic strategies to control the organization of large sets of molecules having a wide compositional and interactional diversity.[1] To this end, the notions of orthogonal self-assembly[2] and self-sorting[3–7] are cornerstones of these strategies, especially when applied within the context of constitutional dynamic chemistry (CDC), based on molecules capable of adapting their constitution by exchange of their reversibly linked components.[1l–n,8,9]

By addressing chemical systems at both molecular and supramolecular levels, CDC provides a convenient way to organize complex dynamic systems and consequently to control their properties. Constitutional dynamic libraries (CDLs) operating *via* the reversible condensation of amine- and 2-formylpyridine-containing components into dynamic imine-based constituents acting as ligands for transition metal cations have unlocked the path toward architectures that would otherwise be inaccessible by traditional synthetic means and/or capable of displaying complex properties (*e.g.* feedback loops, adaptation, *etc.*).[7e–i,9b–e,10,11] It was shown that the simultaneous assembly of several types of such constitutional dynamic architectures within the same reaction mixture allowed for the emergence of new properties going beyond those of each individual architecture,[1n,6d,9d,e,11a–d,q] highlighting a link between increased compositional diversity and diversification of the displayed properties. However, to date, the compositional diversities of "poly-architecture" constitutional dynamic systems are limited. The systems reported in the literature involve architectures which always have at least one or two reagents in common (*i.e.* organic components and/or type of metal cations),[3,6,7] thus limiting their potential in terms of compositional diversification and properties. One major hurdle in the development of more diverse systems is the lack of strategies to simultaneously control the outcome of two (or more) interconnected dynamic processes over several architectures, namely reversible covalent imine bond formation and dynamic metal–ligand coordination.

Here we investigate the simultaneous generation of 11 different pairs of fully non-identical imine-based metal complexes *via* the self-sorting of their six initial building blocks. The study provides insights into the factors influencing the

[a]*Institute of Nanotechnology, Karlsruhe Institute of Technology, 76344 Eggenstein-Leopoldshafen, Germany*

[b]*Laboratoire de Chimie Supramoléculaire, Institut de Science et d'Ingénierie Supramoléculaires, Université de Strasbourg, 8 allée Gaspard Monge, 67000 Strasbourg, France. E-mail: lehn@unistra.fr*

† Electronic supplementary information (ESI) available. See DOI: 10.1039/c9sc04988f

fidelity and the rate of such self-sorting processes and points at the interplay between thermodynamic driving forces and kinetic traps in the self-assembly of constitutional dynamic systems.

Results and discussion

Rationale and initial design

Factors such as the denticity, the steric bulk and the electronic properties of a ligand can be exploited to tune its binding strength with a given type of transition metal, as each transition metal has well-defined coordination preferences due to its unique electronic makeup.[12] The formation of a given imine-containing ligand constituent from a library of amine and aldehyde components can be selectively promoted *via* its preferential binding to one type of transition metal, if this constituent offers the best coordination environment for this metal cation out of all the possible combinations of the initial components.[1f–n,8,9] The same principle can be extended to the simultaneous but selective generation of two (or more) imine-containing ligand constituents if two (or more) types of transition metals having different coordination preferences are used.[9e,f]

A difference between metals of tetrahedral and octahedral coordination geometries exploitable by appropriate ligand design is that the former can be considered to involve two orthogonal planes containing two donor atoms whereas the latter involves two orthogonal planes with three donor atoms. Thus, by choosing amine and aldehyde reactants giving either a planar bidentate or a planar tridentate chelate by imine condensation, selectivity results in that full coordination of the former forms a tetrahedral species while that of the latter yields an octahedral one. When the donor atoms of both ligands are similar (or identical) and the concentrations of both are the same, the higher denticity of the tridentate ligand should lead to a chelate-type binding[13] strongly favouring its binding to a metal ion of octahedral coordination geometry. For such reasons, the condensation of aniline derivative **1** (Fig. 1) with 2-formylpyridine was expected to give a ligand suited to coordination of the tetrahedral Cu(I) center, while condensation of the aminoquinoline derivative **2** was expected to give a ligand suited to coordination of the octahedral Fe(II) center.

The pairing of Fe(II) with one of the two derivatives of 2-formylpyridine can be inhibited by manipulating the steric hindrance around the coordination site of its pyridine. The coordination of the three nitrogen nuclei of 2,2′:6′2″-terpyridine-like ligands—such as the ligands obtained by the condensation of aminoquinoline **2** with derivatives of 2-formylpyridine—to an octahedral metal ion is known to induce a "pinching" of these ligands resulting in a contraction of the distance between their positions 6 and 6″. Any congestion in these positions will destabilize the resulting complex.[14] Consequently, Fe(II) should favor the inclusion of 2-formylpyridine **3** (Fig. 1) in its coordination sphere as it bears less steric hindrance than its peer **4**.

This rationale was tested by mixing components **1**, **2**, **3** and **4** in a 2 : 2 : 2 : 2 ratio in the presence of 1 eq. of $Fe(BF_4)_2$ and 1 eq. of $Cu(BF_4)$ in CD_3CN (Fig. 1). After 18 h at 60 °C, the ^1H NMR spectrum of the crude mixture (Fig. 1, upper part) was not consistent with the complete self-sorting of the initial reagents into the expected complexes $[Cu(\mathbf{1},\mathbf{4})_2]^+$ and $[Fe(\mathbf{2},\mathbf{3})_2]^{2+}$; the notation (**n**,**m**) refers to the imine-based constituent generated by the condensation of amine **n** with aldehyde **m** (in no specific order). Three different sets of signals were observed. These could be assigned to the homoleptic complexes $[Cu(\mathbf{1},\mathbf{4})_2]^+$ and $[Fe(\mathbf{2},\mathbf{3})_2]^{2+}$ along with the heteroleptic complex $[Fe(\mathbf{2},\mathbf{3})(\mathbf{2},\mathbf{4})]^{2+}$. The homo- and heteroleptic Fe(II) complexes formed in a 0.9 : 1 ratio. The homoleptic complex $[Fe(\mathbf{2},\mathbf{4})_2]^{2+}$ containing two sterically hindered pyridine ligands **4** was not observed, attesting to its lower stability compared to the other two Fe(II) complexes.

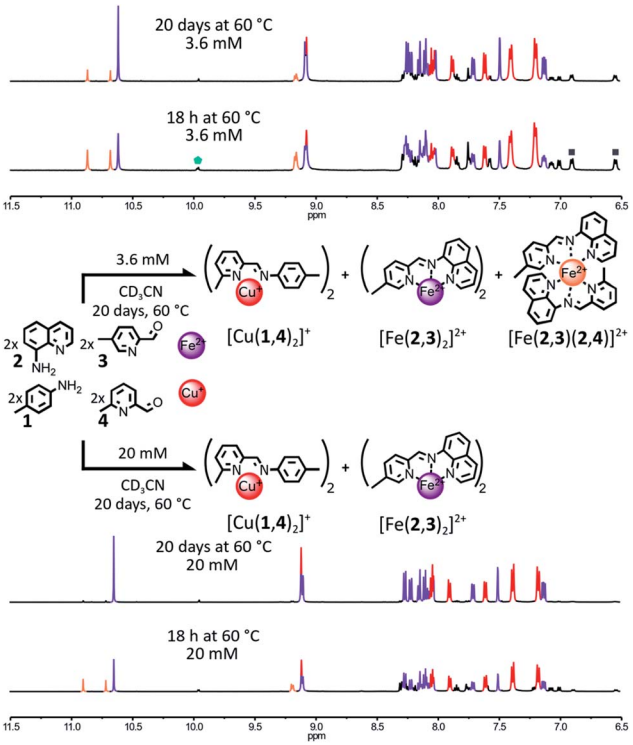

Fig. 1 Simultaneous generation of complexes $[Cu(\mathbf{1},\mathbf{4})_2]^+$ and $[Fe(\mathbf{2},\mathbf{3})_2]^{2+}$ through the self-sorting of their initial reactants. For clarity, the components **1** and **3** and the Cu(I) ions not incorporated into a complex have been omitted from the representation. Top – Reaction conditions: **1** : **2** : **3** : **4** : $Cu(BF_4)$: $Fe(BF_4)_2$ (2 : 2 : 2 : 2 : 1 : 1), 3.6 mM, CD_3CN, 60 °C, up to 20 days. Partial ^1H NMR spectrum (400 MHz, CD_3CN, 297 K) of the crude reaction mixture after 18 h and 20 days at 60 °C. Bottom – Reaction conditions: **1** : **2** : **3** : **4** : $Cu(BF_4)$: $Fe(BF_4)_2$ (2 : 2 : 2 : 2 : 1 : 1), 20 mM, CD_3CN, 60 °C, up to 20 days. The partial ^1H NMR spectrum (400 MHz, CD_3CN, 297 K) of the crude reaction mixture after 18 h and 20 days at 60 °C. Diagnostic signals of the complexes are colour coded, $[Cu(\mathbf{1},\mathbf{4})_2]^+$ in red and $[Fe(\mathbf{2},\mathbf{3})_2]^{2+}$ in purple and $[Fe(\mathbf{2},\mathbf{3})(\mathbf{2},\mathbf{4})]^{2+}$ in orange. One of the diagnostic signals of the free aldehydes **3** and **4** is highlighted by a green pentagon, and two of the diagnostic signals of the free amine **1** are highlighted by grey squares.

Upon further heating of the reaction at 60 °C (Fig. 1, upper part, and ESI, Fig. S51†), the ^1H NMR signals of $[Fe(\mathbf{2},\mathbf{3})(\mathbf{2},\mathbf{4})]^{2+}$ started to fade. The disappearance of the heteroleptic complex

was correlated with an increase in the population of $[Cu(\mathbf{1},\mathbf{4})_2]^+$ and $[Fe(\mathbf{2},\mathbf{3})_2]^{2+}$, hinting that the formation of $[Fe(\mathbf{2},\mathbf{3})(\mathbf{2},\mathbf{4})]^{2+}$ is under kinetic control. However, after 20 days at 60 °C, $[Fe(\mathbf{2},\mathbf{3})(\mathbf{2},\mathbf{4})]^{2+}$ was still present in the reaction mixture, with a homo-to heteroleptic Fe(II) complex ratio of 1 : 0.25. Under these conditions (60 °C, 20 days) this system is not under thermodynamic control, resulting in an incomplete self-sorting process. Thermodynamic control over the assembling of the system could be re-established by concentrating the reaction mixture. At 20 mM (up from 3.6 mM), $[Fe(\mathbf{2},\mathbf{3})(\mathbf{2},\mathbf{4})]^{2+}$ was fully converted into $[Cu(\mathbf{1},\mathbf{4})_2]^+$ and $[Fe(\mathbf{2},\mathbf{3})_2]^{2+}$ after 20 days at 60 °C, with the ^{1}H NMR spectrum of the reaction mixture being a superimposition of the spectra of the isolated complexes $[Cu(\mathbf{1},\mathbf{4})_2]^+$ and $[Fe(\mathbf{2},\mathbf{3})_2]^{2+}$ (Fig. 1, lower part and ESI, Fig. S54†).

To probe the driving forces governing the selective generation of $[Cu(\mathbf{1},\mathbf{4})_2]^+$ and $[Fe(\mathbf{2},\mathbf{3})_2]^{2+}$ at 20 mM, the formation of each one of the two complexes was attempted by mixing 1 eq. of the appropriate metal salt with a 2 : 2 : 2 : 2 mixture of **1**, **2**, **3**, **4** in CD_3CN at 60 °C (ESI, Fig. S55 and S56†). The two reaction mixtures were monitored by ^{1}H NMR spectroscopy over the course of 20 days.

When Fe(II) was added to the organic components, the affinity of Fe(II) for the imine ligand (**2**,**3**) was strong enough to ensure the exclusive formation of one Fe(II) complex after 18 h at 60 °C, $[Fe(\mathbf{2},\mathbf{3})_2]^{2+}$ (ESI, Fig. S56†), whereas when Cu(I) was added alone to the four organic components, $[Cu(\mathbf{1},\mathbf{4})_2]^+$ did not form. Instead, an ill-defined Cu(I) complex was obtained (ESI, Fig. S55†). This result shows that $[Cu(\mathbf{1},\mathbf{4})_2]^+$ is not the thermodynamically most stable Cu(I) complex attainable from the initial library of components but instead constituent (**1**,**4**) is imposed upon Cu(I) by default *via* the ligand selection of Fe(II). Consequently, the formation of the thermodynamic product $[Fe(\mathbf{2},\mathbf{3})_2]^{2+}$ is the main driving force of this self-sorting processes. Similar results were obtained at 3.6 mM (ESI, Fig. S52 and S53†).

This system exemplifies how agonistic amplification between two constituents of a constitutional dynamic network can be exploited to force the expression of a product.[1f–n,8,9] It also confirms the validity of our initial design principles as, at a concentration of 20 mM, two fully non-identical metal complexes could be generated *via* the self-sorting of their initial components. However, it also exposed one major shortcoming of this strategy. At a lower concentration range (2.7–3.6 mM), the slower rearrangement of an intermediate generated under kinetic control (namely, the heteroleptic complex $[Fe(\mathbf{2},\mathbf{3})(\mathbf{2},\mathbf{4})]^{2+}$) trapped the system out-of-equilibrium—and thus out of a sorted outcome—for a length of time limiting the applicability of this type of system. This shortcoming could be addressed by refining the design of the initial library of components so that the rearrangement of this intermediate would be accelerated or its formation prevented.

Influence of the electronic parameters of the initial components on the fidelity of the self-sorting process

The influence of the electronic properties of the organic components on the output of their self-assembly in the presence of Fe(II) and Cu(I) was probed by modifying the electron-donating ability of the 4-substituent of aniline **1** or of the 6-substituent of 2-formylpyridine **4**.

The use of a more electron-rich aniline residue should generate a more stable Cu(I) complex[15] and as complexes $[Fe(\mathbf{2},\mathbf{3})(\mathbf{2},\mathbf{4})]^{2+}$ and $[Cu(\mathbf{1},\mathbf{4})_2]^+$ share the same aldehyde component **4**, the formation of a more stable Cu(I) complex may hamper the formation of $[Fe(\mathbf{2},\mathbf{3})(\mathbf{2},\mathbf{4})]^{2+}$. This hypothesis was tested by replacing the amine component **4** with the more electron rich *N*,*N*-dimethylaminoaniline **5** in the initial library of components (Fig. 2).

When components **2**, **3**, **4**, **5**, $Cu(BF_4)$ and $Fe(BF_4)_2$ were mixed in a 2 : 2 : 2 : 2 : 1 : 1 ratio in CD_3CN, the self-sorting of the system was clearly apparent in the ^{1}H NMR spectrum of the crude mixture. After 3 days at 60 °C, only the diagnostic signals of the two homoleptic complexes $[Fe(\mathbf{2},\mathbf{3})_2]^{2+}$ and $[Cu(\mathbf{4},\mathbf{5})_2]^+$ were observed in the spectrum. The two complexes were generated in an almost perfect 1 : 1 ratio. The use of the electron rich aniline **5** did not inhibit the generation of the kinetic intermediate $[Fe(\mathbf{2},\mathbf{3})(\mathbf{2},\mathbf{4})]^{2+}$. When the self-assembly of $[Fe(\mathbf{2},\mathbf{3})_2]^{2+}$ and $[Cu(\mathbf{4},\mathbf{5})_2]^+$ was followed over time by ^{1}H NMR, the diagnostic signals of $[Fe(\mathbf{2},\mathbf{3})(\mathbf{2},\mathbf{4})]^{2+}$ were immediately detectable upon mixing of the reactants (ESI, Fig. S58†). After 90 min of heating at 60 °C, the amount of $[Fe(\mathbf{2},\mathbf{3})(\mathbf{2},\mathbf{4})]^{2+}$ in solution reached its peak. From this point onward, $[Fe(\mathbf{2},\mathbf{3})(\mathbf{2},\mathbf{4})]^{2+}$ slowly faded whereas the population of $[Fe(\mathbf{2},\mathbf{3})_2]^{2+}$ and $[Cu(\mathbf{4},\mathbf{5})]^+$ kept on increasing for the next 60 h (ESI, Fig. S60†). After 60 h at 60 °C, only the diagnostic signals of the two homoleptic complexes remained visible in the ^{1}H NMR spectra of the crude reaction mixture (ESI, Fig. S59†). While **5** did not prevent the formation of $[Fe(\mathbf{2},\mathbf{3})(\mathbf{2},\mathbf{4})]^{2+}$, it considerably enhanced the rate of redistribution of its components.

The formation of $[Fe(\mathbf{2},\mathbf{3})(\mathbf{2},\mathbf{4})]^{2+}$ could also be impeded by making the sterically hindered 2-formylpyridine **4** a poorer ligand. To do so, the methyl group of **4** was replaced with a slightly bigger and electron withdrawing CF_3 group (Fig. 3). The addition of 1 eq. of $Fe(BF_4)_2$ and 1 eq. of $Cu(BF_4)$ to a 2 : 2 : 2 : 2 mixture of components **1**, **2**, **3**, **6** in CD_3CN

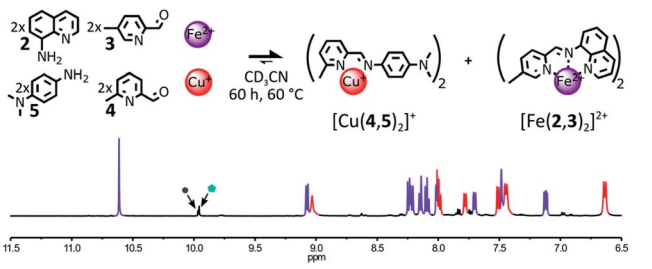

Fig. 2 Top – Simultaneous generation of complexes $[Cu(\mathbf{4},\mathbf{5})_2]^+$ and $[Fe(\mathbf{2},\mathbf{3})_2]^{2+}$ through the self-sorting of their initial reactants. Reaction conditions: **1** : **3** : **4** : **5** : $Cu(BF_4)$: $Fe(BF_4)_2$ (2 : 2 : 2 : 2 : 1 : 1), CD_3CN, 60 °C, 18 h. Bottom – Partial ^{1}H NMR spectrum (400 MHz, CD_3CN, 297 K) of the crude reaction mixture after 18 h at 60 °C, diagnostic signals of the complexes are colour coded, $[Cu(\mathbf{4},\mathbf{5})_2]^+$ in red, $[Fe(\mathbf{2},\mathbf{3})_2]^{2+}$ in purple, one of the diagnostic signals of the free aldehyde **3** is highlighted by a grey circle and one of the diagnostic signals of the free aldehyde **4** is highlighted by a green pentagon.

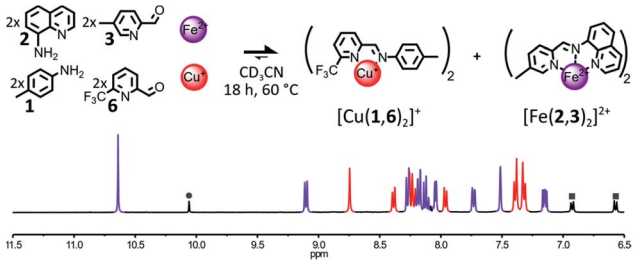

Fig. 3 Top – Generation of complexes $[Cu(\mathbf{1},\mathbf{6})_2]^+$ and $[Fe(\mathbf{2},\mathbf{3})_2]^{2+}$ through the self-sorting of their initial reactants. For clarity, the components **1** and **6** and the Cu(I) ions not incorporated in a complex are omitted from the representation. Reaction conditions: **1** : **2** : **3** : **6** : $Cu(BF_4)$: $Fe(BF_4)_2$ (2 : 2 : 2 : 2 : 1 : 1), CD_3CN, 60 °C, 18 h. Bottom – Partial ^1H NMR spectrum (400 MHz, CD_3CN, 297 K) of the crude reaction mixture after 18 h at 60 °C, the diagnostic signals of the complexes are colour coded, $[Cu(\mathbf{1},\mathbf{6})_2]^+$ in red and $[Fe(\mathbf{2},\mathbf{3})_2]^{2+}$ in purple, one of the diagnostic signals of the free aldehyde **6** is highlighted by a grey circle and diagnostic signals of the free aniline **1** are highlighted by grey squares.

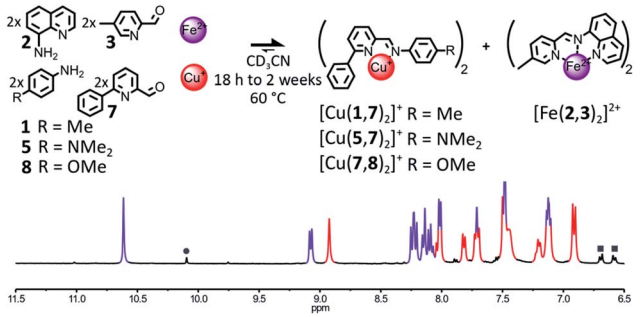

Fig. 4 Top – Generation of complexes $[Cu(\mathbf{X},\mathbf{7})_2]^+$ (X = **1** or **5** or **8**) and $[Fe(\mathbf{2},\mathbf{3})_2]^{2+}$ through the self-sorting of their initial reactants. When amine **1** was used, trace amounts of the heteroleptic complex $[Fe(\mathbf{2},\mathbf{3})(\mathbf{2},\mathbf{7})]^{2+}$ were still observable even after 2 weeks at 60 °C. Reaction conditions: **1** or **5** or **8** : **2** : **3** : **7** : $Cu(BF_4)$: $Fe(BF_4)_2$ (2 : 2 : 2 : 2 : 1 : 1), CD_3CN, 60 °C, 18 h to 2 weeks. Bottom – Partial ^1H NMR spectrum (400 MHz, CD_3CN, 297 K) of the crude reaction mixture after 18 h at 60 °C. The diagnostic signals of the complexes are colour coded, $[Cu(\mathbf{7},\mathbf{8})_2]^+$ in red and $[Fe(\mathbf{2},\mathbf{3})_2]^{2+}$ in purple; one of the diagnostic signals of the free aldehyde **7** is highlighted by a grey circle and two of the diagnostic signals of aniline **8** are highlighted by grey squares.

prompted a rapid self-sorting of the reactants into a 1 : 1 mixture of complexes $[Fe(\mathbf{2},\mathbf{3})_2]^{2+}$ and $[Cu(\mathbf{1},\mathbf{6})_2]^+$ in 18 h at 60 °C (see Fig. 3). The binding abilities of **6** were sufficiently weakened by the introduction of the CF_3 group so that any Fe(II) complex containing it was swiftly converted into $[Fe(\mathbf{2},\mathbf{3})_2]^{2+}$. However, the improvement of the rate of the self-sorting process came at the expense of the stability of the Cu(I) complex generated (ESI, Section 2.2.9†).

Influence of the steric properties of the initial components on the self-sorting process

The influence of the steric hindrance borne by the organic components on the outcome of their self-assembly in the presence of Fe(II) and Cu(I) was investigated by modulating the bulkiness of the substituents ortho to the nitrogens of the pyridine nucleus of aminoquinoline **2** and 2-formylpyridine **4**. The incorporation of a phenyl ring in place of the methyl group of 2-formylpyridine **4** yielded the bulkier aldehyde **7** (Fig. 4). In most cases, the enhanced steric congestion brought by the phenyl ring of **7** was sufficient to prevent the subsistence of the heteroleptic complex $[Fe(\mathbf{2},\mathbf{3})(\mathbf{2},\mathbf{7})]^{2+}$ at equilibrium.

When a 2 : 2 : 2 : 2 mixture of **2**, **3**, **7** and **8** in CD_3CN was treated with 1 eq. of $Cu(BF_4)$ and 1 eq. of $Fe(BF_4)_2$, $[Cu(\mathbf{7},\mathbf{8})_2]^+$ and $[Fe(\mathbf{2},\mathbf{3})_2]^{2+}$ were the only two complexes observable in the ^1H NMR of the reaction mixture after 18 h at 60 °C (1 : 1 ratio, Fig. 4). A similar result was obtained when aniline **5** was used in place of **8** (ESI, Fig. S64†). During the monitoring of the organization of these two libraries by ^1H NMR at 60 °C, both self-sorting processes were found to operate *via* the generation under kinetic control of the heteroleptic complex $[Fe(\mathbf{2},\mathbf{3})(\mathbf{2},\mathbf{7})]^{2+}$ (ESI, Fig. S65, S66 and S69, S70†). $[Fe(\mathbf{2},\mathbf{3})(\mathbf{2},\mathbf{7})]^{2+}$ was immediately generated following the addition of Cu(I) and Fe(II) to the libraries **2**, **3**, **7**, **8** or **2**, **3**, **5**, **7**. Its concentration quickly peaked after 6 min and 1 h, respectively, before gradually declining for the remaining of the experiment. In both cases after 13 h, most of the $[Fe(\mathbf{2},\mathbf{3})(\mathbf{2},\mathbf{7})]^{2+}$ had rearranged and the two desired homoleptic complexes had mostly reached their final concentrations. The incorporation of a phenyl ring in place of the methyl group of **4** did not prevent the formation of $[Fe(\mathbf{2},\mathbf{3})(\mathbf{2},\mathbf{7})]^{2+}$, but significantly increased the rate of its rearrangement. Thermodynamic equilibrium was reached in only 13 h in the case of the library **2**, **3**, **5**, **7** compared to 3 days in the case of the library **2**, **3**, **4**, **5**.

When Cu(I) and Fe(II) were added alone to the library **2**, **3**, **5**, **7**, $[Fe(\mathbf{2},\mathbf{3})_2]^{2+}$ could form whereas $[Cu(\mathbf{5},\mathbf{7})_2]^+$ could not, indicating that, here again, the generation of $[Fe(\mathbf{2},\mathbf{3})_2]^{2+}$ is the main driving force of the self-sorting process (ESI, Fig. S67†).

When the electron poorer aniline **1** was used in place of **5** or **8** in the initial library of components, the heteroleptic complex $[Fe(\mathbf{2},\mathbf{3})(\mathbf{2},\mathbf{7})]^{2+}$ was still observable in the reaction mixture after 2 weeks of heating at 60 °C (ESI, Fig. S62 and S63†), yielding $[Fe(\mathbf{2},\mathbf{3})(\mathbf{2},\mathbf{7})]^{2+}$, $[Fe(\mathbf{2},\mathbf{3})_2]^{2+}$ and $[Cu(\mathbf{1},\mathbf{7})_2]^+$ in a 0.08 : 1 : 0.86 ratio. As free aldehyde **1** was also observed in solution, in a proportion corresponding to that of the missing Cu(I) complex, the lower amount for $[Cu(\mathbf{1},\mathbf{7})_2]^+$ compared to $[Fe(\mathbf{2},\mathbf{3})_2]^{2+}$ could be explained by the partial hydrolysis of imine (**1**,**7**) due to prolonged heating. By itself, the use of the bulkier 2-formylpyridine **7** did not accelerate significantly the redistribution of the components of $[Fe(\mathbf{2},\mathbf{3})(\mathbf{2},\mathbf{7})]^{2+}$ into $[Cu(\mathbf{1},\mathbf{7})_2]^+$ and $[Fe(\mathbf{2},\mathbf{3})_2]^{2+}$. Even in the presence of **7**, the assistance of a derivative of aniline more basic than **1** (such as **5** or **8**) is required to obtain a time efficient self-sorting process.

The destabilization of the Fe(II) heteroleptic complex needs not originate solely from the impairment of the binding abilities of a single one of its components. Instead, milder destabilizing features could be spread through several of its components, so that each one of these features would have a lower effect on the binding abilities of the component bearing it, but the concurrent incorporation of several of them into the same complex would be disfavored. If 6-methylpyridine **4** is reintroduced into the initial library of components in place of **7**,

the formation of $[Fe(\mathbf{2},\mathbf{3})(\mathbf{2},\mathbf{4})]^{2+}$ could be hindered by introducing a methyl group *ortho* to the nitrogen atom of aminoquinoline **2**, such as in **9** (Fig. 5).

An equimolar mixture of components **3**, **4**, **8** and **9** (2 : 2 : 2 : 2) was found to self-sort into the two homoleptic complexes $[Cu(\mathbf{4},\mathbf{8})_2]^+$ and $[Fe(\mathbf{3},\mathbf{9})_2]^{2+}$ after being treated with 1 eq. of $Cu(BF_4)$ and 1 eq. of $Fe(BF_4)_2$ (Fig. 5) in CD_3CN and left to react at 60 °C overnight. The ^{1}H NMR signals of the two complexes were the only ones visible in the spectrum of the crude reaction mixture after 18 h. The two complexes were generated in the expected 1 : 1 ratio. Some of the ^{1}H NMR signals of $[Fe(\mathbf{3},\mathbf{9})_2]^{2+}$ were strongly shifted downfield compared to those of $[Fe(\mathbf{2},\mathbf{3})_2]^{2+}$, indicating that $[Fe(\mathbf{3},\mathbf{9})_2]^{2+}$ must adopt a more distorted octahedral coordination geometry due to the bulkier aminoquinoline **9**.

The incorporation of both the sterically demanding components aminoquinoline **9** and 2-formylpyridine **7** into the initial library markedly improved the rate of the self-sorting process by preventing the generation of the heteroleptic complex $[Fe(\mathbf{3},\mathbf{9})(\mathbf{7},\mathbf{9})]^{2+}$.

Upon the treatment of a 2 : 2 : 2 : 2 mixture of **3**, **7**, **8** and **9** in CD_3CN with 1 eq. of Fe(II) and 1 eq. of Cu(I), the formation of the complexes $[Fe(\mathbf{3},\mathbf{9})_2]^{2+}$ and $[Cu(\mathbf{7},\mathbf{8})_2]^+$ was complete (in the sense that no further changes in the ^{1}H NMR spectrum were detectable) after about 100 min of heating at 60 °C (ESI, Fig. S72–S74†). During the monitoring by ^{1}H NMR of the self-sorting of $[Fe(\mathbf{3},\mathbf{9})_2]^{2+}$ and $[Cu(\mathbf{7},\mathbf{8})_2]^+$, the formation of the heteroleptic complex $[Fe(\mathbf{3},\mathbf{9})(\mathbf{7},\mathbf{9})]^{2+}$ was not observed (ESI, Fig. S73†). The greater steric hindrance of aminoquinoline **9** compared to **2** is likely to disfavor the inclusion of **7** in the same Fe(II) complex, allowing for a quick establishment of the thermodynamic equilibrium state of the system.

A correlation between the prominence of the structural features guiding the self-assembly of the libraries and the rate of their self-sorting process became apparent (ESI, Fig. S75†). (i) When both sterically demanding components aminoquinoline **9** and 2-formylpyridine **7** were incorporated into the initial library, the generation of $[Fe(\mathbf{3},\mathbf{9})_2]^{2+}$ and $[Cu(\mathbf{7},\mathbf{8})_2]^+$ from **3**, **7**, **8** and **9** took 100 min at 60 °C. (ii) In the absence of aminoquinoline **9** the formation of $[Fe(\mathbf{2},\mathbf{3})_2]^{2+}$ and $[Cu(\mathbf{7},\mathbf{8})_2]^+$ from **2**, **3**, **7** and **8** took 800 min under similar conditions. (iii) In the absence of both bulky components, the self-sorting of $[Fe(\mathbf{2},\mathbf{3})_2]^{2+}$ and $[Cu(\mathbf{4},\mathbf{5})_2]^+$ from **2**, **3**, **4** and **5** took 60 h at 60 °C. Such influence of steric effects on the kinetics of a self-assembly process, allowing for quicker establishment of the thermodynamic equilibrium state, deserves further exploration in view of its interest for the design of complex dynamic systems.

Influence of the nature of the metal cation connectors on the self-sorting process

The influence of the coordination preferences of the metal cations triggering the self-sorting process on its fidelity was studied by altering the nature of either the tetracoordinated metal cation used or the hexacoordinated one. We have shown earlier that a library composed of components **2**, **3**, **7** and **8** was able to self-sort into $[Cu(\mathbf{7},\mathbf{8})_2]^+$ and $[Fe(\mathbf{2},\mathbf{3})_2]^{2+}$ when treated with the appropriate metal salts (Fig. 4). Now, the same library of components was treated with either a combination of Ag(I) and Fe(II) or a combination of Cu(I) and Zn(II).

The addition of 1 eq. Ag(I) and 1 eq. Fe(II) to a 2 : 2 : 2 : 2 mixture of **2**, **3**, **7** and **8** in CD_3CN resulted almost exclusively in the formation of the two expected homoleptic complexes $[Ag(\mathbf{7},\mathbf{8})_2]^+$ and $[Fe(\mathbf{2},\mathbf{3})_2]^{2+}$ in a 1 : 1 ratio after 18 h at 60 °C (Fig. 6). In the ^{1}H NMR spectrum of the crude reaction mixture, only small traces of hydrolysis of the constituent (**7**,**8**) were observable besides the two complexes. Such an outcome corroborates our hypothesis that the formation of the octahedral complex is the main driving force of the self-sorting of the library. Thus, the nature of the tetracoordinated metal cation employed has little influence on the outcome of the self-sorting process and Ag(I) could be used in place of Cu(I). Conversely, the substitution of Fe(II) for Zn(II) was found to have more dramatic effects on the output of the self-sorting process.

When 1 eq. of $Zn(BF_4)_2$ and 1 eq. of $Cu(BF_4)$ were mixed with an equimolar mixture of **2**, **3**, **7** and **8** (2 : 2 : 2 : 2) in CD_3CN, the ^{1}H NMR spectra of the crude reaction mixture revealed the formation of four different complexes after 18 h at 60 °C (Fig. 7A). Besides $[Cu(\mathbf{7},\mathbf{8})_2]^+$, the three Zn(II) complexes $[Zn(\mathbf{2},\mathbf{7})_2]^{2+}$, $[Zn(\mathbf{2},\mathbf{3})(\mathbf{2},\mathbf{7})]^{2+}$ and $[Zn(\mathbf{2},\mathbf{3})_2]^{2+}$ were obtained in

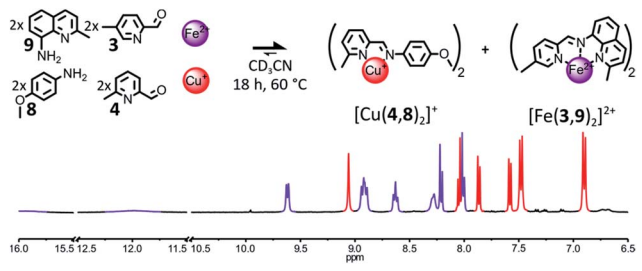

Fig. 5 Top – Generation of complexes $[Cu(\mathbf{4},\mathbf{8})_2]^+$ and $[Fe(\mathbf{3},\mathbf{9})_2]^{2+}$ through the self-sorting of their initial reactants. Reaction conditions: **3** : **4** : **8** : **9** : $Cu(BF_4)$: $Fe(BF_4)_2$ (2 : 2 : 2 : 2 : 1 : 1), CD_3CN, 60 °C, 18 h. Bottom – Partial ^{1}H NMR spectrum (400 MHz, CD_3CN, 297 K) of the crude reaction mixture after 18 h at 60 °C. The diagnostic signals of the complexes are colour coded, $[Cu(\mathbf{4},\mathbf{8})_2]^+$ in red and $[Fe(\mathbf{3},\mathbf{9})_2]^{2+}$ in purple.

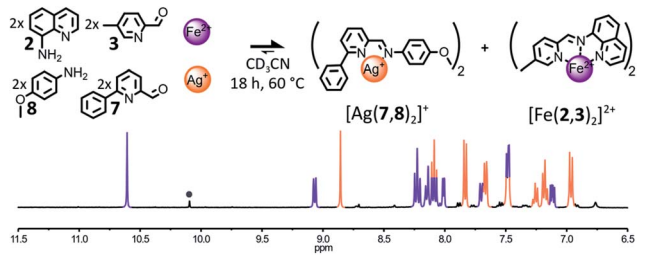

Fig. 6 Top – Generation of complexes $[Ag(\mathbf{7},\mathbf{8})_2]^+$ and $[Fe(\mathbf{2},\mathbf{3})_2]^{2+}$ through the self-sorting of their initial reactants. Reaction conditions: **2** : **3** : **7** : **8** : $Ag(BF_4)$: $Fe(BF_4)_2$ (2 : 2 : 2 : 2 : 1 : 1), CD_3CN, 60 °C, 18 h. Bottom – Partial ^{1}H NMR spectrum (400 MHz, CD_3CN, 297 K) of the crude reaction mixture after 18 h at 60 °C. The diagnostic signals of the complexes are colour coded, $[Ag(\mathbf{7},\mathbf{8})_2]^+$ in orange and $[Fe(\mathbf{2},\mathbf{3})_2]^{2+}$ in purple; one of the diagnostic signals of the free aldehyde **7** is designated by a grey circle.

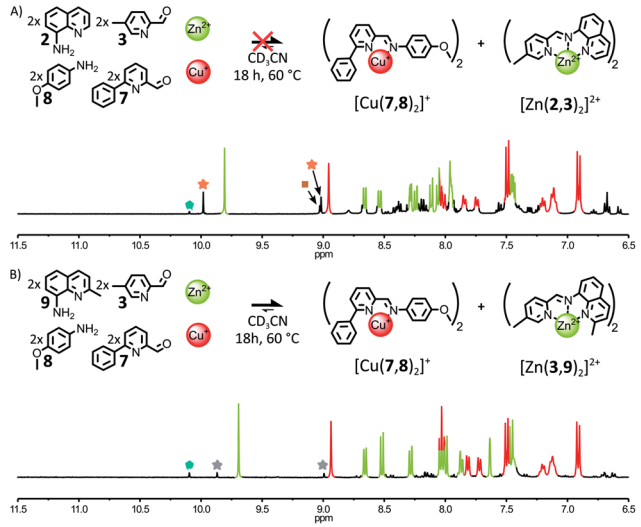

Fig. 7 (A) Top – Attempted generation of complexes $[Cu(\mathbf{7},\mathbf{8})_2]^+$ and $[Zn(\mathbf{2},\mathbf{3})_2]^{2+}$ through the self-sorting of their initial reactants. Reaction conditions: **2** : **3** : **7** : **8** : $Cu(BF_4)$: $Zn(BF_4)_2$ (2 : 2 : 2 : 2 : 1 : 1), CD_3CN, 60 °C, 18 h. Bottom – Partial ^1H NMR spectrum (400 MHz, CD_3CN, 297 K) of the crude reaction mixture after 18 h at 60 °C; the diagnostic signals of the complexes are colour coded, $[Cu(\mathbf{7},\mathbf{8})_2]^+$ in red and $[Zn(\mathbf{2},\mathbf{3})_2]^{2+}$ in green. Two of the diagnostic signals of $[Zn(\mathbf{2},\mathbf{3})(\mathbf{2},\mathbf{7})]^{2+}$ are highlighted by orange stars, one of the diagnostic signals of $[Zn(\mathbf{2},\mathbf{7})_2]^{2+}$ is highlighted by a brown square and one of the diagnostic signals of the free aldehyde **7** is highlighted by a green pentagon. (B) Top – Generation of complexes $[Cu(\mathbf{7},\mathbf{8})_2]^+$ and $[Zn(\mathbf{3},\mathbf{9})_2]^{2+}$ through the self-sorting of their initial reagents. Reaction conditions: **3** : **7** : **8** : **9** : $Cu(BF_4)$: $Zn(BF_4)_2$ (2 : 2 : 2 : 2 : 1 : 1), CD_3CN, 60 °C, 18 h. Bottom – Partial ^1H NMR spectrum (400 MHz, CD_3CN, 297 K) of the crude reaction mixture after 18 h at 60 °C; the diagnostic signals of the complexes are colour coded, $[Cu(\mathbf{7},\mathbf{8})_2]^+$ in red and $[Zn(\mathbf{3},\mathbf{9})_2]^{2+}$ in green. Two of the diagnostic signals of $[Zn(\mathbf{3},\mathbf{9})(\mathbf{7},\mathbf{9})]^{2+}$ are highlighted by grey stars and one of the diagnostic signals of the free aldehyde **7** is highlighted by a green pentagon.

a 0.07 : 0.27 : 1 ratio. Further heating of the reaction mixture at 60 °C for up to 5 days did not change this outcome (ESI, Fig. S78†). The reduced fidelity of this self-sorting process could be explained by the more flexible and accommodating coordination of d^{10} Zn(II) compared to low-spin d^6 Fe(II).[12] Thus, the disparities in energy between $[Zn(\mathbf{2},\mathbf{7})_2]^{2+}$, $[Zn(\mathbf{2},\mathbf{3})(\mathbf{2},\mathbf{7})]^{2+}$ and $[Zn(\mathbf{2},\mathbf{3})_2]^{2+}$—induced by the steric and electronic properties of **2**, **3** and **7**—became insufficient to guide the system towards the exclusive generation of $[Zn(\mathbf{2},\mathbf{3})_2]^{2+}$. Indeed, when 1 eq. of Zn(II) was added to a 2 : 2 : 2 mixture of **2**, **3**, **7** (ESI, Fig. S79 and S80†), $[Zn(\mathbf{2},\mathbf{7})_2]^{2+}$, $[Zn(\mathbf{2},\mathbf{3})(\mathbf{2},\mathbf{7})]^{2+}$ and $[Zn(\mathbf{2},\mathbf{3})_2]^{2+}$ were generated in a 0.05 : 0.21 : 1 ratio after 2 days at 60 °C. This outcome did not change upon further heating of the mixture at 60 °C for up to 6 days. In contrast, when the bulkier aminoquinoline **9** was used in place of **2**, the addition of 1 eq. of Zn(II) to a 2 : 2 : 2 mixture of **3**, **7**, **9** yielded almost exclusively $[Zn(\mathbf{3},\mathbf{9})_2]^{2+}$, after 2 days at 60 °C (ESI, Fig. S82†). These results indicate that stronger assembly instructions in the initial components of the system can offset the more accommodating coordination of Zn(II). When an equimolar mixture of **3**, **7**, **8**, **9** (2 : 2 : 2 : 2) was treated with 1 eq. of $Zn(BF_4)_2$ and 1 eq. of $Cu(BF_4)$ in CD_3CN, the fidelity of the self-sorting process was largely restored (Fig. 7B). After 18 h at 60 °C, the diagnostic signals of complexes $[Cu(\mathbf{7},\mathbf{8})_2]^+$ and $[Zn(\mathbf{3},\mathbf{9})_2]^{2+}$ dominated the ^1H NMR spectrum of the crude reaction mixture. $[Zn(\mathbf{3},\mathbf{9})(\mathbf{7},\mathbf{9})]^{2+}$ was still observed in the reaction mixture but in a lower 0.1 : 1 ratio with $[Zn(\mathbf{3},\mathbf{9})_2]^{2+}$. $[Zn(\mathbf{7},\mathbf{9})_2]^{2+}$ was not detectable. The above systems highlight the correlation existing between the narrowness of the coordination preferences of the metal ions used to drive the self-assembly of a system and the amount of instructions required in the organic components of this system to guide it towards a specific outcome.

Conclusions

The unique coordination preferences of tetrahedral and octahedral metal cations can be exploited to drive the self-sorting of two amine components and two 2-formylpyridine components into two fully non-identical metal complexes of imine ligands.

The fidelity of the self-sorting of the two metal complexes was determined by the capacity of the octahedral metal ion to select its pair of components from the initial pool of reactants, with the ligand of the weaker tetrahedral metal ions being dictated by the components discarded by the octahedral metal ions. The present study stresses the pivotal role of the kinetic intermediates of the various processes involved in the generation of the thermodynamic products of metal ion-driven dynamic covalent systems in reaching a given self-sorted outcome. The concentration, the electronic properties and the steric properties of the initial components of the system were all found to be crucial parameters to manipulate for avoiding kinetic trapping during the sorting of the system. The present study also illustrates how modest alterations of the coordination and/or structural features guiding the self-assembly of the systems can tip the balance between a sorted and disordered final output.

We anticipate that the information gleaned from our investigation will facilitate the design and the manipulation of complex CDNs of molecules having a wide compositional and interactional diversity, an important step towards rivalling with the mastery of biological systems at organizing and exploiting dynamic networks of molecules.

Conflicts of interest

There are no conflicts to declare.

Acknowledgements

The authors acknowledge the financial support by the ERC (Advanced Research Grant SUPRADAPT 290585). JFA acknowledges the financial support by the European Union's Horizon 2020 research and innovation programme under the Marie Skłodowska-Curie grant agreement No 749351. JFA gratefully acknowledges Prof. Jack Harrowfield, Dr Jean-Louis Schmitt and Cyril Antheaume for extensive discussions.

Notes and references

1 For selected resources on the self-organization of chemical systems: (*a*) G. M. Whitesides and R. F. Ismagilov, *Science*, 1999, **284**, 89–92; (*b*) G. M. Whitesides and B. A. Grzybowski, *Science*, 2002, **295**, 2418–2421; (*c*) J.-M. Lehn, *Science*, 2002, **295**, 2400–2403; (*d*) J.-M. Lehn, *Proc. Natl. Acad. Sci. U. S. A.*, 2002, **99**, 4763–4768; (*e*) D. Newth and J. Finnigan, *Aust. J. Chem.*, 2006, **59**, 841–848; (*f*) J.-M. Lehn, *Chem. Soc. Rev.*, 2007, **36**, 151–160; (*g*) M. Schmittel and K. Mahata, *Angew. Chem., Int. Ed.*, 2008, **47**, 5284–5286; (*h*) J. R. Nitschke, *Nature*, 2009, **462**, 736–738; (*i*) M. D. Ward and P. R. Raithbyb, *Chem. Soc. Rev.*, 2013, **42**, 1619–1636; (*j*) G. Ashkenasy, T. M. Hermans, S. Otto and A. F. Taylor, *Chem. Soc. Rev.*, 2017, **46**, 2543–2554; (*k*) T. Kosikova and D. Philp, *Chem. Soc. Rev.*, 2017, **46**, 7274–7305; (*l*) J.-M. Lehn, *Angew. Chem., Int. Ed.*, 2013, **52**, 2836–2850; (*m*) J.-M. Lehn, *Angew. Chem., Int. Ed.*, 2015, **54**, 3276–3289; (*n*) J.-F. Ayme and J.-M. Lehn, *Adv. Inorg. Chem.*, 2018, **71**, 3–78.

2 For selected general resources on orthogonal self-assembly: (*a*) W. T. S. Huck, R. Hulst, P. Timmerman, F. C. J. M. van Veggel and D. N. Reinhoudt, *Angew. Chem., Int. Ed.*, 1997, **36**, 1006–1008; (*b*) V. Goral, M. I. Nelen, A. Eliseev and J.-M. Lehn, *Proc. Natl. Acad. Sci. U. S. A.*, 2001, **98**, 1347–1352; (*c*) M. L. Saha, S. De, S. Pramanikw and M. Schmittel, *Chem. Soc. Rev.*, 2013, **42**, 6860–6909; (*d*) X.-Y. Hu, T. Xiao, C. Lin, F. Huang and L. Wang, *Acc. Chem. Res.*, 2014, **47**, 2041–2051; (*e*) A. Wilson, G. Gasparini and S. Matile, *Chem. Soc. Rev.*, 2014, **43**, 1948–1962; (*f*) P. Wei, X. Yan and F. Huang, *Chem. Soc. Rev.*, 2015, **44**, 815–832.

3 For selected general resources on self-sorting: (*a*) R. Kramer, J.-M. Lehn and A. Marquis-Rigault, *Proc. Natl. Acad. Sci. U. S. A.*, 1993, **90**, 5394–5398; (*b*) S. J. Rowan, D. G. Hamilton, P. A. Brady and J. K. M. Sanders, *J. Am. Chem. Soc.*, 1997, **119**, 2578–2579; (*c*) A. Wu and L. Isaacs, *J. Am. Chem. Soc.*, 2003, **125**, 4831–4835; (*d*) K. Osowska and O. Š. Miljanić, *Synlett*, 2011, 1643–1648; (*e*) M. M. Safont-Sempere, G. Fernández and F. Würthner, *Chem. Rev.*, 2011, **111**, 5784–5814; (*f*) M. L. Saha and M. Schmittel, *Org. Biomol. Chem.*, 2012, **10**, 4651–4684; (*g*) Q. Ji, R. C. Lirag and O. Š. Miljanić, *Chem. Soc. Rev.*, 2014, **43**, 1873–1884; (*h*) Z. He, W. Jiang and C. A. Schalley, *Chem. Soc. Rev.*, 2015, **44**, 779–789; (*i*) W. Wang, Y.-X. Wang and H.-B. Yang, *Chem. Soc. Rev.*, 2016, **45**, 2656–2693; (*j*) C.-W. Hsu and O. Š. Miljanić, in *Dynamic Covalent Chemistry: Principles, Reactions, and Applications*, ed. W. Zhang and Y. Jin, Wiley, 2017; (*k*) M. Schmittel and S. Saha, *Adv. Inorg. Chem.*, 2018, **71**, 135–176; (*l*) S. Saha, I. Regeni and G. H. Clever, *Coord. Chem. Rev.*, 2018, **374**, 1–14.

4 For selected examples of self-sorting processes based on dynamic covalent bonds: (*a*) J. W. Sadownik and D. Philp, *Angew. Chem., Int. Ed.*, 2008, **47**, 9965–9970; (*b*) B. Içli, N. Christinat, J. Tönnemann, C. Schüttler, R. Scopelliti and K. Severin, *J. Am. Chem. Soc.*, 2009, **131**, 3154–3155; (*c*) P. Vongvilai and O. Ramström, *J. Am. Chem. Soc.*, 2009, **131**, 14419–14425; (*d*) K. Osowska and O. Š. Miljanić, *J. Am. Chem. Soc.*, 2011, **133**, 724–727; (*e*) Q. Ji and O. Š. Miljanić, *J. Org. Chem.*, 2013, **78**, 12710–12716; (*f*) C. W. Hsu and O. Š. Miljanić, *Angew. Chem., Int. Ed.*, 2015, **54**, 2219–2222; (*g*) S. Klotzbach and F. Beuerle, *Angew. Chem., Int. Ed.*, 2015, **54**, 10356–10360.

5 For selected examples of self-sorting processes based on metal complexes: (*a*) P. N. W. Baxter, J.-M. Lehn, A. DeCian and J. Fischer, *Angew. Chem., Int. Ed.*, 1993, **32**, 69–72; (*b*) D. L. Caulder and K. N. Raymond, *Angew. Chem., Int. Ed.*, 1997, **36**, 1440–1442; (*c*) P. N. Taylor and H. L. Anderson, *J. Am. Chem. Soc.*, 1999, **121**, 11538–11545; (*d*) C. Addicott, N. Das and P. J. Stang, *Inorg. Chem.*, 2004, **43**, 5335–5338; (*e*) Y. R. Zheng, H. B. Yang, K. Ghosh, L. Zhao and P. J. Stang, *Chem.–Eur. J.*, 2009, **15**, 7203–7214; (*f*) A. M. Johnson and R. J. Hooley, *Inorg. Chem.*, 2011, **50**, 4671–4673; (*g*) X. Lu, X. Li, K. Guo, T.-Z. Xie, C. N. Moorefield, C. Wesdemiotis and G. R. Newkome, *J. Am. Chem. Soc.*, 2014, **136**, 18149–18155; (*h*) W. M. Bloch, J. J. Holstein, W. Hiller and G. H. Clever, *Angew. Chem., Int. Ed.*, 2017, **56**, 8285–8289.

6 For selected examples of self-sorting processes based on constitutional dynamic metal complexes: (*a*) D. Schultz and J. R. Nitschke, *Angew. Chem., Int. Ed.*, 2006, **45**, 2453–2456; (*b*) M. Schmittel, M. L. Saha and J. Fan, *Org. Lett.*, 2011, **13**, 3916–3919; (*c*) C. J. Campbell, D. A. Leigh, I. J. Vitorica-Yrezabal and S. L. Woltering, *Angew. Chem., Int. Ed.*, 2014, **53**, 13771–13774; (*d*) A. Jiménez, R. A. Bilbeisi, T. K. Ronson, S. Zarra, C. Woodhead and J. R. Nitschke, *Angew. Chem., Int. Ed.*, 2014, **53**, 4556–4560; (*e*) J.-F. Ayme, J. E. Beves, C. J. Campbell and D. A. Leigh, *Angew. Chem., Int. Ed.*, 2014, **53**, 7823–7827; (*f*) L. R. Holloway, M. C. Young, G. J. Beran and R. J. Hooley, *Chem. Sci.*, 2015, **6**, 4801–4806; (*g*) A. M. Johnson, C. A. Wiley, M. C. Young, X. Zhang, Y. Lyon, R. R. Julian and R. J. Hooley, *Angew. Chem., Int. Ed.*, 2015, **54**, 5641–5645; (*h*) C. A. Wiley, L. R. Holloway, T. F. Miller, Y. Lyon, R. R. Julian and R. J. Hooley, *Inorg. Chem.*, 2016, **55**, 9805–9815; (*i*) L. R. Holloway, P. M. Bogie and R. J. Hooley, *Dalton Trans.*, 2017, **46**, 14719–14723.

7 For selected examples on self-sorting processes involving supramolecular architectures built around more than one type of metal template: (*a*) X. Sun, D. W. Johnson, D. L. Caulder, R. E. Powers, K. N. Raymond and E. H. Wong, *Angew. Chem., Int. Ed.*, 1999, **38**, 1303–1307; (*b*) F. Ibukuro, M. Fujita, K. Yamagushi and J.-P. Sauvage, *J. Am. Chem. Soc.*, 1999, **121**, 11014–11015; (*c*) K. Mahata and M. Schmittel, *J. Am. Chem. Soc.*, 2009, **131**, 16544–16554; (*d*) K. Mahata, M. L. Saha and M. Schmittel, *J. Am. Chem. Soc.*, 2010, **132**, 15933–15935; (*e*) M. M. Smulders, A. Jiménez and J. R. Nitschke, *Angew. Chem., Int. Ed.*, 2012, **51**, 6681–6685; (*f*) M. L. Saha and M. Schmittel, *J. Am. Chem. Soc.*, 2013, **135**, 17743–17746; (*g*) M. L. Saha, N. Mittal, J. W. Bats and M. Schmittel, *Chem. Commun.*, 2014, **50**, 12189–12192; (*h*) W. J. Ramsay, F. T. Szczypinski, H. Weissman, T. K. Ronson, M. M. J. Smulders, B. Rybtchinski and J. R. Nitschke, *Angew. Chem., Int. Ed.*,

2015, **54**, 5636–5640; (*i*) F. J. Rizzuto, W. J. Ramsay and J. R. Nitschke, *J. Am. Chem. Soc.*, 2018, **140**, 11502–11509; (*j*) M. D. Wise, J. J. Holstein, P. Pattison, C. Besnard, E. Solari, R. Scopelliti, G. Bricogne and K. Severin, *Chem. Sci.*, 2015, **6**, 1004–1010; (*k*) H. Sepehrpour, M. L. Saha and P. J. Stang, *J. Am. Chem. Soc.*, 2017, **139**, 2553–2556; (*l*) S. Gaikwad, M. L. Saha, D. Samanta and M. Schmittel, *Chem. Commun.*, 2017, **53**, 8034–8037.

8 For selected general resources on constitutional dynamic chemistry: (*a*) J.-M. Lehn, *Top. Curr. Chem.*, 2012, **322**, 1–32; (*b*) *Constitutional Dynamic Chemistry, Topics in Current Chemistry*, ed. M. Barboiu, Springer, Berlin, 2012, vol. 322.

9 For selected recent examples of applications of constitutional dynamic chemistry: (*a*) N. Hafezi and J. -M. Lehn, *J. Am. Chem. Soc.*, 2012, **134**, 12861–12868; (*b*) G. Vantomme, S. Jiang and J.-M. Lehn, *J. Am. Chem. Soc.*, 2014, **136**, 9509–9518; (*c*) J. Holub, G. Vantomme and J.-M. Lehn, *J. Am. Chem. Soc.*, 2016, **138**, 11783–11791; (*d*) S. Dhers, J. Holub and J.-M. Lehn, *Chem. Sci.*, 2017, **8**, 2125–2130; (*e*) G. Men and J.-M. Lehn, *J. Am. Chem. Soc.*, 2017, **139**, 2474–2483; (*f*) P. Kovaricek, A. C. Meister, K. Flidrova, R. Cabot, K. Kovarickova and J.-M. Lehn, *Chem. Sci.*, 2016, **7**, 3215–3226; (*g*) O. Shyshov, R.-C. Brachvogel, T. Bachmann, R. Srikantharajah, D. Segets, F. Hampel, R. Puchta and M. von Delius, *Angew. Chem., Int. Ed.*, 2017, **56**, 776–781; (*h*) H. Löw, E. Mena-Osteritz and M. von Delius, *Chem. Sci.*, 2018, **9**, 4785–4793.

10 For selected examples of the complexity of the metallo-supramolecular architectures reachable from amine-and 2-formylpyridine-containing components: (*a*) K. S. Chichak, S. J. Cantrill, A. R. Pease, S.-H. Chiu, G. W. V. Cave, J. L. Atwood and J. F. Stoddart, *Science*, 2004, **304**, 1308–1312; (*b*) J. R. Nitschke, *Acc. Chem. Res.*, 2007, **40**, 103–112; (*c*) J.-F. Ayme, J. E. Beves, D. A. Leigh, R. T. McBurney, K. Rissanen and D. Schultz, *Nat. Chem.*, 2012, **4**, 15–20; (*d*) J.-F. Ayme, J. E. Beves, D. A. Leigh, R. T. McBurney and D. Schultz, *J. Am. Chem. Soc.*, 2012, **134**, 9488–9497; (*e*) J. E. Beves, C. J. Campbell, D. A. Leigh and R. G. Pritchard, *Angew. Chem., Int. Ed.*, 2013, **52**, 6464–6467; (*f*) C. S. Wood, T. K. Ronson, A. M. Belenguer, J. J. Holstein and J. R. Nitschke, *Nat. Chem.*, 2015, **7**, 354–358.

11 For selected examples of the functional potential of metallosupramolecular architecture built from amine-and 2-formylpyridine-containing components: *potential for adaptation to stimuli*, see ref. 9 and (*a*) V. E. Campbell, X. de Hatten, N. Delsuc, B. Kauffmann, I. Huc and J. R. Nitschke, *Nat. Chem.*, 2010, **2**, 684–687; (*b*) A. J. McConnell, C. S. Wood, P. P. Neelakandan and J. R. Nitschke, *Chem. Rev.*, 2015, **115**, 7729–7793; (*c*) B. S. Pilgrim, D. A. Roberts, T. G. Lohr, T. K. Ronson and J. R. Nitschke, *Nat. Chem.*, 2017, **9**, 1276–1281; (*d*) D. A. Roberts, B. S. Pilgrim and J. R. Nitschke, *Chem. Soc. Rev.*, 2018, **47**, 626–644; (*e*) S. Pramanik and I. Aprahamian, *J. Am. Chem. Soc.*, 2016, **138**, 15142–15145; (*f*) L. R. Holloway, H. H. McGarraugh, M. C. Young, W. Sontising, G. J. O. Beran and R. J. Hooley, *Chem. Sci.*, 2016, **7**, 4423–4427; (*g*) D. A. Roberts, B. S. Pilgrim, G. Sirvinskaite, T. K. Ronson and J. R. Nitschke, *J. Am. Chem. Soc.*, 2018, **140**, 9616–9623; potential as molecular containers; (*h*) P. Mal, B. Breiner, K. Rissanen and J. R. Nitschke, *Science*, 2009, **324**, 1697–1699; (*i*) T. K. Ronson, S. Zarra, S. P. Black and J. R. Nitschke, *Chem. Commun.*, 2013, **49**, 2476–2490; (*j*) A. G. Salles Jr, S. Zarra, R. M. Turner and J. R. Nitschke, *J. Am. Chem. Soc.*, 2013, **135**, 19143–19146; (*k*) S. Zarra, D. M. Wood, D. A. Roberts and J. R. Nitschke, *Chem. Soc. Rev.*, 2015, **44**, 419–432; potential as biologically active molecules or as a mimic of biological molecules; (*l*) A. C. G. Hotze, N. J. Hodges, R. E. Hayden, C. Sanchez-Cano, C. Paines, N. Male, M.-K. Tse, C. M. Bunce, J. K. Chipman and M. J. Hannon, *Chem. Biol.*, 2008, **15**, 1258–1267; (*m*) T. R. Cook, V. Vajpayee, M. H. Lee, P. S. Stang and K. W. Chi, *Acc. Chem. Res.*, 2013, **46**, 2464–2474; (*n*) A. D. Faulkner, R. A. Kaner, Q. M. A. Abdallah, G. Clarkson, D. J. Fox, P. Gurnani, S. E. Howson, R. M. Phillips, D. I. Roper, D. H. Simpson and P. Scott, *Nat. Chem.*, 2014, **6**, 797–803; (*o*) R. Kaner, S. Allison, A. Faulkner, R. Phillips, D. Roper, S. Shepherd, D. Simpson, N. Waterfield and P. Scott, *Chem. Sci.*, 2016, **7**, 951–958; potential as polymeric materials; (*p*) C.-F. Chow, S. Fujii and J.-M. Lehn, *Angew. Chem., Int. Ed.*, 2007, **46**, 5007–5010; (*q*) C.-F. Chow, S. Fujii and J.-M. Lehn, *Chem.–Asian J.*, 2008, **3**, 1324–1335; (*r*) G. Schaeffer, E. Buhler, S. J. Candau and J.-M. Lehn, *Macromolecules*, 2013, **46**, 5664–5671; (*s*) S. Ulrich and J.-M. Lehn, *Angew. Chem., Int. Ed.*, 2008, **47**, 2240–2243; (*t*) S. Ulrich, E. Buhler and J.-M. Lehn, *New J. Chem.*, 2009, **33**, 271–292; (*u*) S. Ulrich and J.-M. Lehn, *J. Am. Chem. Soc.*, 2009, **131**, 5546–5559; potential as anion binders; (*v*) I. A. Riddell, T. K. Ronson, J. K. Clegg, C. S. Wood, R. A. Bilbeisi and J. R. Nitschke, *J. Am. Chem. Soc.*, 2014, **136**, 9491–9498; (*w*) J.-F. Ayme, J. E. Beves, C. J. Campbell, G. Gil-Ramírez, D. A. Leigh and A. J. Stephens, *J. Am. Chem. Soc.*, 2015, **137**, 9812–9815; (*x*) R. A. Bilbeisi, T. Prakasam, M. Lusi, R. El-Khoury, C. Platas-Iglesias, L. J. Charbonnière, J.-C. Olsen, M. Elhabiri and A. Trabolsi, *Chem. Sci.*, 2016, **7**, 2524–2532.

12 *Comprehensive Coordination Chemistry II*, ed, J. A. McCleverty and T. J. Meyer, Elsevier Ltd., 2004.

13 G. Schwarzenbach, *Helv. Chim. Acta*, 1952, **35**, 2344–2363.

14 J.-F. Ayme, J. Lux, J.-P. Sauvage and A. Sour, *Chem.–Eur. J.*, 2012, **18**, 5565–5573.

15 D. Schultz and J. R. Nitschke, *J. Am. Chem. Soc.*, 2006, **128**, 9887–9892.